JOURNAL OF AEROSPACE INFORMATION SYSTEMS
Vol. 16, No. 10, October 2019

Technical Notes

Computational Performance of Complex Spacecraft Simulations Using Back-Substitution

Cody Allard,* Manuel Diaz Ramos,† and Hanspeter Schaub‡
University of Colorado, Boulder, Colorado 80309-0431

DOI: 10.2514/1.I010713

Nomenclature

$B_c, S_i, P_{c,j}$	=	rigid hub, ith solar panel, and jth slosh center of mass location, respectively
$\{\hat{\boldsymbol{b}}_1, \hat{\boldsymbol{b}}_2, \hat{\boldsymbol{b}}_3\}$	=	body frame basis vectors
$\boldsymbol{c}$	=	vector from point B to center of mass of the spacecraft C, m
$\boldsymbol{F}_{\text{ext}}$	=	vector sum of external forces on spacecraft, N
$\{\hat{\boldsymbol{h}}_{i,1}, \hat{\boldsymbol{h}}_{i,2}, \hat{\boldsymbol{h}}_{i,3}\}$	=	ith hinge frame basis vectors
$[I_{\text{sc},B}], [I_{\text{sp}_i,S_i}]$	=	inertia tensor of spacecraft about point B, of solar panel about point S_i, kg $\cdot$ m^2
k_i, c_i	=	ith solar panel torsional spring constant ([N $\cdot$ m]/rad), torsional damping ([N $\cdot$ m $\cdot$ s]/rad)
k_j, c_j	=	jth slosh particle spring constant (N/m), damping ([N $\cdot$ s]/m)
$\boldsymbol{L}_B$	=	vector of sum of external torques of spacecraft about point B, N $\cdot$ m
$m_{\text{sc}}, m_{\text{hub}}, m_{\text{sp}_i}, m_j$	=	mass of spacecraft, hub, ith solar panel, and jth slosh particle, respectively
N, B, H_i, P_j	=	inertial frame origin, body frame origin, ith hinge frame origin, and jth slosh equilibrium point, respectively
$\mathcal{N}, \mathcal{B}, \mathcal{H}_i, \mathcal{S}_i$	=	reference frame of inertial, body, ith hinge, and ith solar panel, respectively
$\boldsymbol{r}_{B/N}$	=	position vector of B with respect to N, m
$\{\hat{\boldsymbol{s}}_{i,1}, \hat{\boldsymbol{s}}_{i,2}, \hat{\boldsymbol{s}}_{i,3}\}$	=	ith solar panel frame basis vectors
θ_i, ρ_j	=	ith solar panel deflection from equilibrium, jth slosh particle displacement
$\boldsymbol{\omega}_{\mathcal{BN}}$	=	angular velocity vector of $\mathcal{B}$ frame with respect to $\mathcal{N}$ frame, deg /s

I. Introduction

SPACECRAFT are becoming more complex, and performance requirements are becoming increasingly more stringent. As a result, simulations of spacecraft need to be of higher fidelity to capture the complex behavior. Often this leads to simulating multibody systems, and some examples of these systems are spacecraft with flexing solar arrays, fuel slosh, and robotic arms. The equations of motion (EOMs) that describe one of these systems result in a nondiagonal system mass matrix that can be difficult to implement in software as the resulting dynamics are fully coupled. Additionally, inverting the system mass matrix or solving the coupled systems of equations using linear algebra techniques can be computationally expensive. Depending on the method used, inverting a dense system mass matrix of size $N \times N$ scales with N^3. However, the computational efficiency depends on the form of the system mass matrix and the numerical methods used to solve the system of equations.

Multibody dynamics has a rich history in the literature especially pertaining to spacecraft applications [1–3]. Furthermore, there are many different methods to derive EOMs that can lead to different forms of the equations [4]. Some forms of the EOMs can be more advantageous than others. For example, using a tree topology to derive the EOMs results in a diagonally dominant system mass matrix [5,6]. This form of the EOMs is advantageous because numerical method techniques can be used to solve system of equations with sparse system mass matrices and increase the computational efficiency [7]. Additionally, Lagrangian mechanics can be used to arrive at diagonally dominant system mass matrices [8]. However, special identities must be used when dealing with attitude parameterization [9] and can be cumbersome with multibody dynamics formulations. In contrast, spacial operator algebra can be used to form a diagonally dominant system mass matrix [10], and a recursive algorithm exists that corresponds to this form of the EOMs and shows to be more computationally efficient than inverting the full system mass matrix [11].

All of the methods described result in populating a system mass matrix. However, populating such a matrix and managing the interrelations between different models can result in disorganized software and can be difficult to maintain [12]. In Ref. [12], a new modular software architecture is introduced that uses an analytical back-substitution method to one-way decouple the EOMs while still solving the full system dynamics. This enables complex spacecraft systems to be modeled in a modular manner in software frameworks such as the Basilisk astrodynamics software where the user does not have to re-derive the EOMs, but is able to selectively activate spacecraft dynamic effectors such as flexing panels, imbalanced reaction wheels, or fuel slosh particles. A couple of benefits of the back-substitution method are that it avoids the

Received 15 December 2018; revision received 14 July 2019; accepted for publication 25 July 2019; published online 5 September 2019.

*Graduate Research Assistant, Department of Aerospace Engineering Sciences, 431 UCB, Colorado Center for Astrodynamics Research. Student Member AIAA.

†Graduate Research Assistant, Department of Aerospace Engineering Sciences, 431 UCB, Colorado Center for Astrodynamics Research.

‡Professor, Glenn L. Murphy Endowed Chair, Department of Aerospace Engineering Sciences, 431 UCB, Colorado Center for Astrodynamics Research. Associate Fellow AIAA.

necessity to populate and manage full system mass matrix and allows the coupled EOMs to be implemented in a modular fashion. Even though this is advantageous from a software implementation perspective, the computational efficiency needs to be quantified in comparison to use an efficient linear algebra solver. Reference [12] demonstrates that this back-substitution method is achievable for a spacecraft system if the dynamic effectors are all linked through a rigid spacecraft hub component, and not directly linked to each other. Thus, hinged panels are attached to the hub and not to each other. This paper studies the computational efficiency of this back-substitution method in contrast to developing the full system matrix and using a linear algebra solver to solve for the inverse. Two effectors with vastly different algebraic complexity are chosen to see how the effector complexity impacts the back-substitution speed up factor. The EOMs and back-substitution method are developed for a spacecraft with lumped mass fuel slosh (simple dynamic effector) and flexing appended bodies (complex dynamic effector). Of interest is how the complexity of the analytical back-substitution impacts the computational speed of this method in contrast to a computational linear algebra solution.

II. Derivation of Equations of Motion

The back-substitution method introduced in Ref. [12] is generalized for a wide variety of spacecraft applications and needs to be implemented to a specific system to evaluate the computational efficiency of the method. Similar to this paper, multiple publications present models of spacecraft dynamics with appended solar panels [13–15]. Additionally, using modal representations of appended bodies is a common practice to incorporate multiple modes without solving the full continuous flexible body solution. The fuel slosh motion is being approximated by a lumped mechanical multimode model [16,17]. However, the EOMs need to be derived using the systematic approach provided in Ref. [12] to use the back-substitution method. The derivation in this paper for the flexing and fuel slosh dynamics is similar to Ref. [18]. However, this formulation uses Kane's method [4], which is a powerful method used to derive EOMs.

The formulation assumes that there is a rigid-body hub, with N_S solar panels (or appended rigid-bodies) and N_P lumped masses in the tank for the fuel. Subscript i is used to indicate the ith solar panel and subscript j is used to indicate the jth fuel slosh mass, m_j. Figure 1 displays the frame and variable definitions used for this formulation.

There are four coordinate frames defined for this formulation. The inertial reference frame is indicated by $\mathcal{N}$:$\{\hat{\boldsymbol{n}}_1, \hat{\boldsymbol{n}}_2, \hat{\boldsymbol{n}}_3\}$. The body-fixed coordinate frame, $\mathcal{B}$:$\{\hat{\boldsymbol{b}}_1, \hat{\boldsymbol{b}}_2, \hat{\boldsymbol{b}}_3\}$, is anchored to the hub and can be oriented in any direction. The solar panel frame, $\mathcal{S}_i$:$\{\hat{\boldsymbol{s}}_{i,1}, \hat{\boldsymbol{s}}_{i,2}, \hat{\boldsymbol{s}}_{i,3}\}$, has its origin located at its corresponding hinge location, H_i. The $\mathcal{S}_i$ frame is oriented such that $\hat{\boldsymbol{s}}_{i,1}$ points antiparallel to the center of mass of its solar panel, $S_{c,i}$. The $\hat{\boldsymbol{s}}_{i,2}$ axis is defined as the rotation axis that would yield a positive θ_i using the right-hand rule. The distance from point H_i to point S_i is defined as d_i. The hinge frame, $\mathcal{H}_i$:$\{\hat{\boldsymbol{h}}_{i,1}, \hat{\boldsymbol{h}}_{i,2}, \hat{\boldsymbol{h}}_{i,3}\}$, is fixed with respect to the body frame, and is equivalent to the respective $\mathcal{S}_i$ frame when the corresponding solar panel is undeflected.

There are a few more key locations that need to be defined. Point B is the origin of the body frame and can have any location with respect to the hub. Point B_c is the location of the center of mass of the rigid hub. P_j is the undeflected or equilibrium position of each corresponding slosh mass, while point $P_{c,j}$ is the current position of that slosh mass.

Figure 2 provides further detail of the fuel slosh and hinged solar panel parameters. As seen in Fig. 2b, an individual slosh particle is constrained to move along its corresponding $\hat{\boldsymbol{p}}_j$ direction while connected by a spring with a linear spring constant value k_j and by a linear damper with a damping coefficient, c_j. The variable ρ_j is a state variable and quantifies the displacement from equilibrium for the corresponding slosh mass. Analogously, Fig. 2a shows that each solar panel, with mass m_{sp_i}, is connected by a torsional spring with spring constant, $k_{\theta,i}$ and has a rotational damper with coefficient $c_{\theta,i}$. The state variable describing a solar panel's angular displacement from equilibrium is θ_i.

Using the variables and frames defined, the derivation is completed using Kane's method. Kane's method is a powerful tool to derive EOMs because it retains the same systematic approach regardless of the number of degrees of freedom being considered, it does not require the angular momentum expression and its corresponding inertial time derivative, and it arrives at the desired angular velocity form [4,19].

Kane's method begins by defining the state variables and their respective generalized speeds. For this problem, the state variables $\boldsymbol{X}$ and the generalized speeds $\boldsymbol{u}$ can be seen in Eqs. (1) and (2). It should be noted that another benefit of using Kane's method is that the generalized speeds do not need to be the direct inertial time derivative of the state variables [4]. The vector $\boldsymbol{r}_{B/N}$ describes the location from the inertial frame origin to the

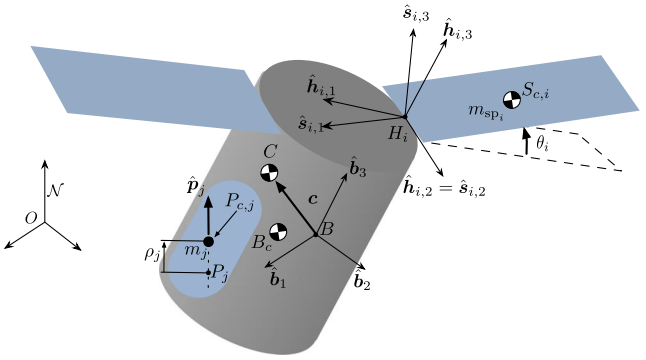

Fig. 1 Frame and variable definitions used for formulation.

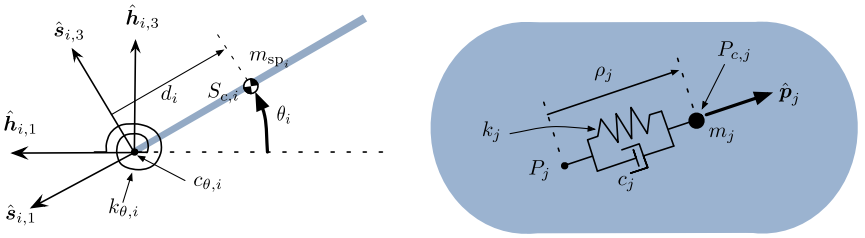

a) Detailed description of single solar panel **b) Detailed description of single slosh particle**

Fig. 2 Further detail of solar panels and fuel slosh.

Table 1 Partial velocity table

r	$\boldsymbol{v}_r^{B_c}$	$\boldsymbol{\omega}_r^{\mathcal{B}}$	$\boldsymbol{v}_r^{S_i}$	$\boldsymbol{\omega}_r^{\mathcal{S}i}$	$\boldsymbol{v}_r^{P_c}$
1–3	$[I_{3\times3}]$	$[0_{3\times3}]$	$[I_{3\times3}]$	$[0_{3\times3}]$	$[I_{3\times3}]$
4–6	$-[\tilde{\boldsymbol{r}}_{B_c/B}]$	$[I_{3\times3}]$	$-[\tilde{\boldsymbol{r}}_{S_i/B}]$	$[I_{3\times3}]$	$-[\tilde{\boldsymbol{r}}_{P_{c,j}/B}]$
$7-(N_S+6)$	$[0_{3\times1}]$	$[0_{3\times1}]$	$d_i\hat{\boldsymbol{s}}_{i,3}$	$\hat{\boldsymbol{s}}_{i,2}$	$[0_{3\times1}]$
$(N_S+7)-(N_S+7+N_P)$	$[0_{3\times1}]$	$[0_{3\times1}]$	$[0_{3\times1}]$	$[0_{3\times1}]$	$\hat{\boldsymbol{p}}_j$

body frame origin and is the translational state for the hub. The set $\boldsymbol{\sigma}_{\mathcal{BN}}$ contains modified Rodrigues parameters (MRPs) describing the attitude of the body frame $\mathcal{B}$ with respect to the inertial frame $\mathcal{N}$. However, it should be noted that the EOMs developed in this paper are independent of the chosen attitude parameterization set, and therefore any attitude parameterization set could be used.

$$\boldsymbol{X} = [\boldsymbol{r}_{B/N} \quad \boldsymbol{\sigma}_{\mathcal{BN}} \quad \theta_1 \quad \cdot \quad \cdot \quad \theta_{N_S} \quad \rho_1 \quad \cdot \quad \cdot \quad \rho_{N_P}]^T \tag{1}$$

$$\boldsymbol{u} = [\dot{\boldsymbol{r}}_{B/N} \quad \boldsymbol{\omega}_{\mathcal{BN}} \quad \dot{\theta}_1 \quad \cdot \quad \cdot \quad \dot{\theta}_{N_S} \quad \dot{\rho}_1 \quad \cdot \quad \cdot \quad \dot{\rho}_{N_P}]^T \tag{2}$$

The angular velocity of the body frame $\mathcal{B}$ with respect to the inertial frame $\mathcal{N}$ is labeled as $\boldsymbol{\omega}_{\mathcal{BN}}$ and is a generalized speed describing the rotational velocity of the rigid hub. In Kane's method there is typically an index r that defines the rth generalized speed. In this paper it is chosen to keep the compact vector notation; therefore, when a vector is defined for the generalized speeds, it corresponds to three generalized speeds. For example, the translational velocity of the hub $\dot{\boldsymbol{r}}_{B/N}$ corresponds to the $r = 1$–3 generalized speeds for this problem.

The next step in Kane's method is to use the generalized states and speeds and define the translational velocity of each body's center of mass, and the angular velocity of each body if it has inertia properties. Before defining these quantities, the notation used in this paper needs to be clarified. Vector notation is taken from Ref. [20]. A time derivative of a vector $\boldsymbol{v}$ with respect to the body frame $\mathcal{B}$ is denoted by $\boldsymbol{v}'$; the inertial time derivative is labeled as $\dot{\boldsymbol{v}}$. This paper expresses vector equations as matrix equations. However, a reference frame in which the matrix components are expressed with respect to is not specified. It should be noted that when implementing these equations in software a single reference frame must be used. A common frame to express the equations is the body frame, $\mathcal{B}$. Because these equations are matrix equations, the following notation is used: the cross product is expressed as $[\tilde{\boldsymbol{a}}]\boldsymbol{b}$, the dot product is expressed as $\boldsymbol{a}^T\boldsymbol{b}$, and the outer product is expressed as $\boldsymbol{a}\boldsymbol{b}^T$.

In this problem, the translational velocity of the center of mass of the rigid-body hub can be computed as

$$\dot{\boldsymbol{r}}_{B_c/N} = \dot{\boldsymbol{r}}_{B/N} + \boldsymbol{\omega}_{\mathcal{BN}} \times \boldsymbol{r}_{B_c/B} = \dot{\boldsymbol{r}}_{B/N} - [\tilde{\boldsymbol{r}}_{B_c/B}]\boldsymbol{\omega}_{\mathcal{BN}} \tag{3}$$

and the rigid-body hub's angular velocity is simply the generalized speed $\boldsymbol{\omega}_{\mathcal{BN}}$.

Similarly, the translational velocity of the center of mass of the ith solar panel is

$$\dot{\boldsymbol{r}}_{S_i/N} = \dot{\boldsymbol{r}}_{B/N} + \boldsymbol{r}'_{S_i/B} + \boldsymbol{\omega}_{\mathcal{BN}} \times \boldsymbol{r}_{S_i/B} = \dot{\boldsymbol{r}}_{B/N} + d_i\dot{\theta}_i\hat{\boldsymbol{s}}_{i,3} - [\tilde{\boldsymbol{r}}_{S_i/B}]\boldsymbol{\omega}_{\mathcal{BN}} \tag{4}$$

and the angular velocity of the ith solar panel is defined as

$$\boldsymbol{\omega}_{\mathcal{S}_i/\mathcal{N}} = \boldsymbol{\omega}_{\mathcal{BN}} + \dot{\theta}_i\hat{\boldsymbol{s}}_{i,2} \tag{5}$$

The fuel slosh particles are assumed to be point masses that do not have inertia properties. Therefore, only the translational velocity of the center of mass of each slosh particle needs to be defined. This definition is shown in Eq. (6).

$$\dot{\boldsymbol{r}}_{P_{c,j}/N} = \dot{\boldsymbol{r}}_{B/N} + \boldsymbol{r}'_{P_{c,j}/B} + \boldsymbol{\omega}_{\mathcal{BN}} \times \boldsymbol{r}_{P_{c,j}/B} = \dot{\boldsymbol{r}}_{B/N} + \dot{\rho}_j\hat{\boldsymbol{p}}_j - [\tilde{\boldsymbol{r}}_{P_{c,j}/B}]\boldsymbol{\omega}_{\mathcal{BN}} \tag{6}$$

Finally, the system's center of mass velocity needs to be defined and can be seen in Eq. (7).

$$\dot{\boldsymbol{r}}_{C/N} = \dot{\boldsymbol{r}}_{B/N} + \dot{\boldsymbol{c}} \tag{7}$$

A crucial step in Kane's method is defining the partial velocities [4] that are used for defining the EOMs. A partial velocity is defined as the partial derivative of a velocity with respect to a generalized speed [4]. To define the notation used, if a rigid body with a center of mass labeled as point A has a frame attached to it labeled as $\mathcal{A}$, then the partial velocity of the center of mass with respect to the rth generalized speed is labeled as v_r^A. The partial velocity of the rotational velocity of frame $\mathcal{A}$ with respect to the rth generalized speed is $\boldsymbol{\omega}_r^A$. Using this notation, the partial velocity table for this problem can be seen Table 1.

An additional partial velocity that is needed is $[\boldsymbol{v}_{1-3}^C]$ for the external force applied on the spacecraft, $\boldsymbol{F}_{\text{ext}}$. Using Eq. (7) the following is defined

$$[\boldsymbol{v}_{1-3}^C] = [I_{3\times3}] \tag{8}$$

Now that the partial velocities are defined, the EOMs can be found using Kane's method. The following section summarizes the translational EOM derivation.

A. Rigid Spacecraft Hub Translational Equations of Motion

Kane's method defines generalized active forces and generalized inertia forces [4]. The definition of a generalized active force can be seen in Eq. (9).

$$F_r = \sum_r^N \boldsymbol{v}_r^T \cdot \boldsymbol{F} \tag{9}$$

where $\boldsymbol{F}$ is a force being applied to the system. Using this definition the external force applied on the spacecraft for the translational equations is defined as

$$\boldsymbol{F}_{1\text{–}3} = [\boldsymbol{v}_{1\text{–}3}^C]^T \boldsymbol{F}_{\text{ext}} = \boldsymbol{F}_{\text{ext}} \tag{10}$$

Next the definition of a generalized inertia force is

$$F_r^* = \sum_r^N [\boldsymbol{\omega}_r^T \boldsymbol{T}^* + \boldsymbol{v}_r^T(-m_r \boldsymbol{a}_r)] \tag{11}$$

where $\boldsymbol{T}^*$ is the generalized inertia torque of a rigid body, $\boldsymbol{a}_r$ is the acceleration of each body's center of mass, and m_r is the corresponding mass value. Using the definition, the generalized inertia forces for the translational motion are

$$\boldsymbol{F}_{1\text{–}3}^* = [\boldsymbol{v}_{1\text{–}3}^{B_c}]^T(-m_{\text{hub}}\ddot{\boldsymbol{r}}_{B_c/N}) + \sum_i^{N_S}[\boldsymbol{v}_{1\text{–}3}^{S_i}]^T(-m_{\text{sp}_i}\ddot{\boldsymbol{r}}_{S_i/N}) + \sum_j^{N_P}[\boldsymbol{v}_{1\text{–}3}^{P_c}]^T(-m_j\ddot{\boldsymbol{r}}_{P_{c,j}/N}) \quad = -m_{\text{hub}}\ddot{\boldsymbol{r}}_{B_c/N} + \sum_i^{N_S} -m_{\text{sp}_i}\ddot{\boldsymbol{r}}_{S_i/N} + \sum_j^{N_P} -m_j\ddot{\boldsymbol{r}}_{P_{c,j}/N} \tag{12}$$

The last definition needed for Kane's method is Kane's equation [4], seen in Eq. (13), which will yield the EOMs of the system.

$$F_r + F_r^* = 0; \qquad r = 1, 2, \ldots N \tag{13}$$

Applying Eq. (13) to the translational motion yields

$$\boldsymbol{F}_{\text{ext}} - m_{\text{hub}}\ddot{\boldsymbol{r}}_{B_c/N} + \sum_i^{N_S} -m_{\text{sp}_i}\ddot{\boldsymbol{r}}_{S_i/N} + \sum_j^{N_P} -m_j\ddot{\boldsymbol{r}}_{P_{c,j}/N} = 0 \tag{14}$$

Expanding the acceleration terms and simplifying results in the following equation:

$$\begin{aligned} &m_{\text{hub}}\ddot{\boldsymbol{r}}_{B/N} + m_{\text{hub}}[\dot{\boldsymbol{\omega}}_{\mathcal{B}/N} \times \boldsymbol{r}_{B_c/B} + \boldsymbol{\omega}_{\mathcal{B}/N} \times (\boldsymbol{\omega}_{\mathcal{B}/N} \times \boldsymbol{r}_{B_c/B})] + \sum_i^{N_S} m_{\text{sp}_i}[\ddot{\boldsymbol{r}}_{B/N} + d_i(\ddot{\theta}_i\hat{\boldsymbol{s}}_{i,3} + \dot{\theta}_i^2\hat{\boldsymbol{s}}_{i,1}) \\ &+2\boldsymbol{\omega}_{\mathcal{B}/N} \times \boldsymbol{r}'_{S_i/B} + \dot{\boldsymbol{\omega}}_{\mathcal{B}/N} \times \boldsymbol{r}_{S_i/B} + \boldsymbol{\omega}_{\mathcal{B}/N} \times (\boldsymbol{\omega}_{\mathcal{B}/N} \times \boldsymbol{r}_{S_i/B})] + \sum_j^{N_P} m_j[\ddot{\boldsymbol{r}}_{B/N} + \ddot{\rho}_j\hat{\boldsymbol{p}}_j \\ &+2\boldsymbol{\omega}_{\mathcal{B}/N} \times \boldsymbol{r}'_{P_{c,j}/B} + \dot{\boldsymbol{\omega}}_{\mathcal{B}/N} \times \boldsymbol{r}_{P_{c,j}/B} + \boldsymbol{\omega}_{\mathcal{B}/N} \times (\boldsymbol{\omega}_{\mathcal{B}/N} \times \boldsymbol{r}_{P_{c,j}/B})] = \boldsymbol{F}_{\text{ext}} \end{aligned} \tag{15}$$

Combining like terms and moving second-order state variables to the left-hand side of the equation

$$m_{\text{sc}}\ddot{\boldsymbol{r}}_{B/N} - m_{\text{sc}}[\tilde{\boldsymbol{c}}]\dot{\boldsymbol{\omega}}_{\mathcal{B}/N} + \sum_i^{N_s} m_{\text{sp}_i} d_i\hat{\boldsymbol{s}}_{i,3}\ddot{\theta}_i + \sum_{j=1}^{N_P} m_j\hat{\boldsymbol{p}}_j\ddot{\rho}_j = \boldsymbol{F}_{\text{ext}} - 2m_{\text{sc}}[\tilde{\boldsymbol{\omega}}_{\mathcal{B}/N}]\boldsymbol{c}' - m_{\text{sc}}[\tilde{\boldsymbol{\omega}}_{\mathcal{B}/N}][\tilde{\boldsymbol{\omega}}_{\mathcal{B}/N}]\boldsymbol{c} - \sum_i^{N_s} m_{\text{sp}_i} d_i\dot{\theta}_i^2\hat{\boldsymbol{s}}_{i,1} \tag{16}$$

Equation (16) is the final form of the translational EOM.

B. Rigid Spacecraft Hub Rotational Equations of Motion

The total external torque acting on the spacecraft $\boldsymbol{L}_B$ needs to be defined as a generalized active force. Using Eq. (9) the generalized active forces acting on the spacecraft for the rotational equations can be defined as

$$\boldsymbol{F}_{4\text{–}6} = [\boldsymbol{\omega}_{4\text{–}6}^{\mathcal{B}}]^T \boldsymbol{L}_B = \boldsymbol{L}_B \tag{17}$$

To compute the generalized inertia forces using Eq. (11), $\boldsymbol{T}^*$ needs to be defined for a rigid body. The following definition applies to both the rigid body hub and each solar panel

$$\boldsymbol{T}^* = -[I_c]\dot{\boldsymbol{\omega}} - [\tilde{\boldsymbol{\omega}}][I_c]\boldsymbol{\omega} \tag{18}$$

Using this definition, the generalized inertia forces for the rotational dynamics are

$$\begin{aligned}\boldsymbol{F}^*_{4\text{–}6} &= [\boldsymbol{\omega}^{\mathcal{B}}_{4\text{–}6}]^T\boldsymbol{T}^*_{\text{hub}} + [\boldsymbol{v}^{B_c}_{4\text{–}6}]^T(-m_{\text{hub}}\ddot{\boldsymbol{r}}_{B_c/N}) + \sum_i^{N_S}([\boldsymbol{v}^{S_i}_{4\text{–}6}]^T(-m_{\text{sp}_i}\ddot{\boldsymbol{r}}_{S_i/N}) + [\boldsymbol{\omega}^{Si}_{4\text{–}6}]^T\boldsymbol{T}^*_{\text{sp}_i})\\ &+ \sum_j^{N_P}[\boldsymbol{v}^{P_c}_{4\text{–}6}]^T(-m_j\ddot{\boldsymbol{r}}_{P_{c,j}/N}) = -[I_{\text{hub},B}]\dot{\boldsymbol{\omega}}_{\mathcal{B}/N} - [\tilde{\boldsymbol{\omega}}_{\mathcal{B}/N}][I_{\text{hub},B}]\boldsymbol{\omega}_{\mathcal{B}/N} - m_{\text{hub}}[\tilde{\boldsymbol{r}}_{B_c/B}]\ddot{\boldsymbol{r}}_{B_c/N}\\ &+ \sum_i^{N_S}(-m_{\text{sp}_i}[\tilde{\boldsymbol{r}}_{S_i/B}]\ddot{\boldsymbol{r}}_{S_i/N} - [I_{\text{sp}_i,S_i}]\dot{\boldsymbol{\omega}}_{\mathcal{S}_{i/N}} - [\tilde{\boldsymbol{\omega}}_{\mathcal{S}_{i/N}}][I_{\text{sp}_i,S_i}]\boldsymbol{\omega}_{\mathcal{S}_{i/N}}) + \sum_j^{N_P}-[\tilde{\boldsymbol{r}}_{P_{c,j}/B}]^T(-m_j\ddot{\boldsymbol{r}}_{P_{c,j}/N})\end{aligned} \tag{19}$$

Now that both the generalized active and inertia forces have been defined, Kane's equation, Eq. (13), is used to obtain the EOMs for the rotational dynamics

$$\begin{aligned}&\boldsymbol{L}_B - [I_{\text{hub},B}]\dot{\boldsymbol{\omega}}_{\mathcal{B}/N} - [\tilde{\boldsymbol{\omega}}_{\mathcal{B}/N}][I_{\text{hub},B}]\boldsymbol{\omega}_{\mathcal{B}/N} - m_{\text{hub}}[\tilde{\boldsymbol{r}}_{B_c/B}]\ddot{\boldsymbol{r}}_{B_c/N} + \sum_i^{N_S}(-m_{\text{sp}_i}[\tilde{\boldsymbol{r}}_{S_i/B}]\ddot{\boldsymbol{r}}_{S_i/N}\\ &-[I_{\text{sp}_i,S_i}]\dot{\boldsymbol{\omega}}_{\mathcal{S}_{i/N}} - [\tilde{\boldsymbol{\omega}}_{\mathcal{S}_{i/N}}][I_{\text{sp}_i,S_i}]\boldsymbol{\omega}_{\mathcal{S}_{i/N}}) + \sum_j^{N_P}-[\tilde{\boldsymbol{r}}_{P_{c,j}/B}]^T(-m_j\ddot{\boldsymbol{r}}_{P_{c,j}/N}) = 0\end{aligned} \tag{20}$$

The rotational dynamics equation requires more extensive simplification. However, these steps are not included here for sake of brevity. Combining like terms and simplifying results in

$$\begin{aligned}&\boldsymbol{L}_B - m_{\text{sc}}[\tilde{\boldsymbol{c}}]\ddot{\boldsymbol{r}}_{B/N} - [I_{\text{sc},B}]\dot{\boldsymbol{\omega}}_{\mathcal{B}/N} - \sum_i^{N_S}[I_{s_{i,2}}\hat{\boldsymbol{s}}_{i,2} + m_{\text{sp}_i}d_i[\tilde{\boldsymbol{r}}_{S_i/B}]\hat{\boldsymbol{s}}_{i,3}]\ddot{\theta}_i - \sum_{j=1}^{N_P}m_j[\tilde{\boldsymbol{r}}_{P_{c,j}/B}]\hat{\boldsymbol{p}}_j\ddot{\rho}_j\\ &-[\tilde{\boldsymbol{\omega}}_{\mathcal{B}/N}][I_{\text{sc},B}]\boldsymbol{\omega}_{\mathcal{B}/N} + \sum_i^{N_S}(-2m_{\text{sp}_i}[\tilde{\boldsymbol{r}}_{S_i/B}][\boldsymbol{\omega}_{\mathcal{B}/N}\times\boldsymbol{r}'_{S_i/B}] - \dot{\theta}_i(I_{s_{i,3}} - I_{s_{i,1}})(\hat{\boldsymbol{s}}_{i,1}\hat{\boldsymbol{s}}^T_{i,3} + \hat{\boldsymbol{s}}_{i,3}\hat{\boldsymbol{s}}^T_{i,1})\boldsymbol{\omega}_{\mathcal{B}/N}\\ &-m_{\text{sp}_i}d_i\dot{\theta}^2_i[\tilde{\boldsymbol{r}}_{S_i/B}]\hat{\boldsymbol{s}}_{i,1} - I_{s_{i,2}}\dot{\theta}_i[\tilde{\boldsymbol{\omega}}_{\mathcal{B}/N}]\hat{\boldsymbol{s}}_{i,2}) - \sum_{j=1}^{N_P}m_j[\tilde{\boldsymbol{\omega}}_{\mathcal{B}/N}][\tilde{\boldsymbol{r}}_{P_{c,j}/B}]\boldsymbol{r}'_{P_{c,j}/B} = 0\end{aligned} \tag{21}$$

Similar to the translational equation, the second-order state variables are moved to the left-hand side of the equation

$$\begin{aligned}&m_{\text{sc}}[\tilde{\boldsymbol{c}}]\ddot{\boldsymbol{r}}_{B/N} + [I_{\text{sc},B}]\dot{\boldsymbol{\omega}}_{\mathcal{B}/N} + \sum_i^{N_S}[I_{s_{i,2}}\hat{\boldsymbol{s}}_{i,2} + m_{\text{sp}_i}d_i[\tilde{\boldsymbol{r}}_{S_i/B}]\hat{\boldsymbol{s}}_{i,3}]\ddot{\theta}_i + \sum_{j=1}^{N_P}m_j[\tilde{\boldsymbol{r}}_{P_{c,j}/B}]\hat{\boldsymbol{p}}_j\ddot{\rho}_j\\ &= -[\tilde{\boldsymbol{\omega}}_{\mathcal{B}/N}][I_{\text{sc},B}]\boldsymbol{\omega}_{\mathcal{B}/N} - [I'_{\text{sc},B}]\boldsymbol{\omega}_{\mathcal{B}/N} - \sum_i^{N_S}(m_{\text{sp}_i}[\tilde{\boldsymbol{\omega}}_{\mathcal{B}/N}][\tilde{\boldsymbol{r}}_{S_i/B}]\boldsymbol{r}'_{S_i/B} + m_{\text{sp}_i}d_i\dot{\theta}^2_i[\tilde{\boldsymbol{r}}_{S_i/B}]\hat{\boldsymbol{s}}_{i,1} + I_{s_{i,2}}\dot{\theta}_i[\tilde{\boldsymbol{\omega}}_{\mathcal{B}/N}]\hat{\boldsymbol{s}}_{i,2})\\ &-\sum_{j=1}^{N_P}m_j[\tilde{\boldsymbol{\omega}}_{\mathcal{B}/N}][\tilde{\boldsymbol{r}}_{P_{c,j}/B}]\boldsymbol{r}'_{P_{c,j}/B} + \boldsymbol{L}_B\end{aligned} \tag{22}$$

Equation (22) is the final form of the rotational dynamics EOM. Now the individual flexing and slosh EOMs need to be computed to fully describe the motion of the system.

C. Hinged Rigid-Body Equations of Motion

Following a similar pattern of the translational and rotational equations, the generalized active forces acting on an individual solar panel are defined as

$$F_7 = \boldsymbol{\omega}^{Si}_r\cdot(-k_i\theta_i\hat{\boldsymbol{s}}_{i,2} - c_i\dot{\theta}_i\hat{\boldsymbol{s}}_{i,2}) = \hat{\boldsymbol{s}}_{i,2}\cdot(-k_i\theta_i\hat{\boldsymbol{s}}_{i,2} - c_i\dot{\theta}_i\hat{\boldsymbol{s}}_{i,2}) = -k_i\theta_i - c_i\dot{\theta}_i \tag{23}$$

The generalized inertia forces are defined accordingly

$$F^*_7 = \boldsymbol{\omega}^{Si}_r\cdot\boldsymbol{T}^*_{\text{sp}_i} + \boldsymbol{v}^{S_i}_r\cdot(-m_{\text{sp}_i}\ddot{\boldsymbol{r}}_{S_i/N}) = \boldsymbol{\omega}^{Si}_r\cdot[-[I_{\text{sp}_i,S_i}]\dot{\boldsymbol{\omega}}_{\mathcal{S}_{i/N}} - [\tilde{\boldsymbol{\omega}}_{\mathcal{S}_{i/N}}][I_{\text{sp}_i,S_i}]\boldsymbol{\omega}_{\mathcal{S}_{i/N}}] + \boldsymbol{v}^{S_i}_r\cdot(-m_{\text{sp}_i}\ddot{\boldsymbol{r}}_{S_i/N}) \tag{24}$$

Using Kane's equation, the EOM for the hinged rigid-bodies can be seen in Eq. (25).

$$-k_i\theta_i - c_i\dot{\theta}_i + \hat{\boldsymbol{s}}_{i,2}\cdot[-[I_{\text{sp}_i,S_i}]\dot{\boldsymbol{\omega}}_{\mathcal{S}_{i/N}} - [\tilde{\boldsymbol{\omega}}_{\mathcal{S}_{i/N}}][I_{\text{sp}_i,S_i}]\boldsymbol{\omega}_{\mathcal{S}_{i/N}}] + d_i\hat{\boldsymbol{s}}_{i,3}\cdot(-m_{\text{sp}_i}\ddot{\boldsymbol{r}}_{S_i/N}) = 0 \tag{25}$$

Expanding and simplifying terms in Eq. (25) yields

$$\begin{aligned}&-m_{\text{sp}_i}d_i\hat{\boldsymbol{s}}_{i,3}\cdot\ddot{\boldsymbol{r}}_{B/N} - [I_{s_i,2}\hat{\boldsymbol{s}}^T_{i,2} - m_{\text{sp}_i}d_i\hat{\boldsymbol{s}}^T_{i,3}[\tilde{\boldsymbol{r}}_{S_i/B}]]\dot{\boldsymbol{\omega}}_{\mathcal{B}/N} - [I_{s_i,2} + m_{\text{sp}_i}d^2_i]\ddot{\theta}_i\\ &-k_i\theta_i - c_i\dot{\theta}_i - (I_{s_{i,1}} - I_{s_{i,3}})\omega_{s_{i,3}}\omega_{s_{i,1}} - m_{\text{sp}_i}d_i\hat{\boldsymbol{s}}_{i,3}\cdot[2\boldsymbol{\omega}_{\mathcal{B}/N}\times\boldsymbol{r}'_{S_i/B} + \boldsymbol{\omega}_{\mathcal{B}/N}\times(\boldsymbol{\omega}_{\mathcal{B}/N}\times\boldsymbol{r}_{S_i/B})] = 0\end{aligned} \tag{26}$$

Finally, the second-order state variables are moved to the left-hand side of the equation:

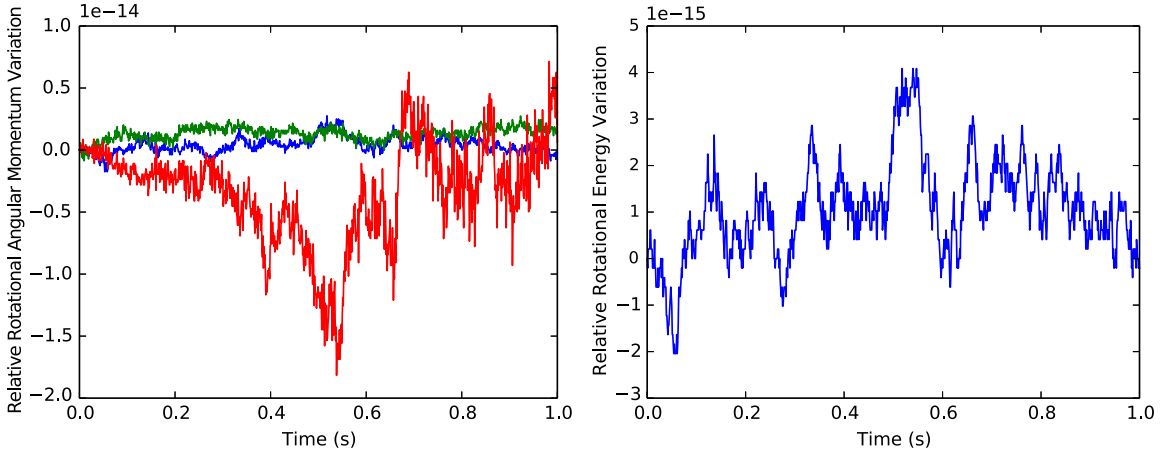

a) Relative change in rotational angular momentum **b) Relative change in rotational energy**

Fig. 3 Simulation verification results for equations of motion.

$$\begin{aligned} &m_{\mathrm{sp}_i} d_i \hat{\boldsymbol{s}}_{i,3}^T \ddot{\boldsymbol{r}}_{B/N} + [I_{s_i,2}\hat{\boldsymbol{s}}_{i,2}^T - m_{\mathrm{sp}_i} d_i \hat{\boldsymbol{s}}_{i,3}^T [\tilde{\boldsymbol{r}}_{S_i/B}]]\dot{\boldsymbol{\omega}}_{\mathcal{B}/N} + [I_{s_i,2} + m_{\mathrm{sp}_i} d_i^2]\ddot{\theta}_i \\ &\quad = -k_i\theta_i - c_i\dot{\theta}_i + (I_{s_{i,3}} - I_{s_{i,1}})\omega_{s_{i,3}}\omega_{s_{i,1}} - m_{\mathrm{sp}_i} d_i \hat{\boldsymbol{s}}_{i,3}^T [\tilde{\boldsymbol{\omega}}_{\mathcal{B}/N}][\tilde{\boldsymbol{\omega}}_{\mathcal{B}/N}]\boldsymbol{r}_{S_i/B} = 0 \end{aligned} \tag{27}$$

Equation (27) is the final form of the EOMs for an individual hinged rigid body. Notice that the second-order state variables for the hub and the current hinged rigid body are present, but the second-order state variables for the other hinged rigid-bodies and the slosh particles are not. This is a key insight and will allow for the back-substitution method introduced in Ref. [12].

D. Fuel Slosh Equations of Motion

Figure 2b shows that a single fuel slosh particle is free to move along its corresponding $\hat{\boldsymbol{p}}_j$ direction and this formulation is generalized to include N_P number of fuel slosh particles. To begin the derivation, the generalized active forces are defined:

$$\boldsymbol{F}_7 = \boldsymbol{v}_r^{P_c} \cdot (-k\rho_j\hat{\boldsymbol{p}}_j - c\dot{\rho}\hat{\boldsymbol{p}}_j) = -k\rho_j - c\dot{\rho} \tag{28}$$

Additionally, the generalized inertia forces are defined as

$$\boldsymbol{F}_7^* = \boldsymbol{v}_r^{P_c} \cdot (-m_j\ddot{\boldsymbol{r}}_{P_{c,j}/N}) = \hat{\boldsymbol{p}}_j^T(-m_j\ddot{\boldsymbol{r}}_{P_{c,j}/N}) \tag{29}$$

Using Kane's equation the following EOMs are obtained:

$$-k\rho_j - c\dot{\rho} - m_j\hat{\boldsymbol{p}}_j^T[\ddot{\boldsymbol{r}}_{B/N} + \ddot{\rho}_j\hat{\boldsymbol{p}}_j + 2\boldsymbol{\omega}_{\mathcal{B}/N}\times\boldsymbol{r}'_{P_{c,j}/B} + \dot{\boldsymbol{\omega}}_{\mathcal{B}/N}\times\boldsymbol{r}_{P_{c,j}/B} \quad + \boldsymbol{\omega}_{\mathcal{B}/N}\times(\boldsymbol{\omega}_{\mathcal{B}/N}\times\boldsymbol{r}_{P_{c,j}/B})] = 0 \tag{30}$$

Combining like terms, moving second-order state variables to the left-hand side, and simplifying results in

$$m_j\hat{\boldsymbol{p}}_j^T\ddot{\boldsymbol{r}}_{B/N} - m_j\hat{\boldsymbol{p}}_j^T[\tilde{\boldsymbol{r}}_{P_{c,j}/B}]\dot{\boldsymbol{\omega}}_{\mathcal{B}/N} + m_j\ddot{\rho}_j = -k_j\rho_j - c_j\dot{\rho}_j - 2m_j\hat{\boldsymbol{p}}_j^T[\tilde{\boldsymbol{\omega}}_{\mathcal{B}/N}]\boldsymbol{r}'_{P_{c,j}/B} - m_j\hat{\boldsymbol{p}}_j^T[\tilde{\boldsymbol{\omega}}_{\mathcal{B}/N}][\tilde{\boldsymbol{\omega}}_{\mathcal{B}/N}]\boldsymbol{r}_{P_{c,j}/B} \tag{31}$$

Equation (31) is the slosh EOM and completes the derivation of the EOM of a spacecraft with N_S appended hinged rigid bodies and N_P fuel slosh particles. When deriving the EOMs of a new system, it is important to verify that the system is agreeing with first principles, and one method to check this is by verifying energy and momentum conservation when applicable. The EOMs of this system were derived in Ref. [18] using Newtonian and Eulerian mechanics and the authors provided energy and momentum checks. The equations presented in this paper were developed using Kane's method and are identical to those seen in Ref. [18]. The conservation of total spacecraft rotational angular momentum and rotational energy is shown in Fig. 3 for the EOMs presented in this paper. These results give confidence in the EOMs and the software implementation. The conservation of energy and momentum results are independent of the spacecraft parameters and initial conditions of the system, which is why these values are not included in the paper. This is the system that the computational performance of the back-substitution method will be tested with. The following section develops the back-substitution form for this system.

III. Back-Substitution Method

The equations presented in the previous sections result in $N_S + N_P + 6$ fully coupled differential equations. Therefore, if the EOMs were placed into state space form, a system mass matrix of size $N_S + N_P + 6$ would need to be inverted or solved using a linear algebra technique to numerically integrate the EOMs using explicit integration techniques. This can result in a computationally expensive simulation. In Ref. [12] the back-substitution method is introduced, and this section shows the implementation of this method for a system with flexing appended bodies and fuel slosh particles.

Following Ref. [12], first both the slosh particles and flexing equations are rearranged so that the second-order state variables are isolated on the left-hand side of the equations. Performing this on the slosh equation yields

$$\ddot{\rho}_j = \frac{1}{m_j}(-m_j\hat{\boldsymbol{p}}_j^T\ddot{\boldsymbol{r}}_{B/N} + m_j\hat{\boldsymbol{p}}_j^T[\tilde{\boldsymbol{r}}_{P_{c,j}/B}]\dot{\boldsymbol{\omega}}_{\mathcal{B}/N} \quad + \hat{\boldsymbol{p}}_j^T\boldsymbol{F}_G - k_j\rho_j - c_j\dot{\rho}_j - 2m_j\hat{\boldsymbol{p}}_j^T[\tilde{\boldsymbol{\omega}}_{\mathcal{B}/N}]\boldsymbol{r}'_{P_{c,j}/B} - m_j\hat{\boldsymbol{p}}_j^T[\tilde{\boldsymbol{\omega}}_{\mathcal{B}/N}][\tilde{\boldsymbol{\omega}}_{\mathcal{B}/N}]\boldsymbol{r}_{P_{c,j}/B}) \tag{32}$$

Equation (32) can be simplified to the following form:

$$\ddot{\rho}_j = \boldsymbol{a}_{\rho_j}^T \ddot{\boldsymbol{r}}_{B/N} + \boldsymbol{b}_{\rho_j}^T \dot{\boldsymbol{\omega}}_{\mathcal{B}/N} + c_{\rho_j} \tag{33}$$

using the definitions seen in Eqs. (34–36).

$$\boldsymbol{a}_{\rho_j} = -\hat{\boldsymbol{p}}_{\boldsymbol{j}} \tag{34}$$

$$\boldsymbol{b}_{\rho_j} = -[\tilde{\boldsymbol{r}}_{P_{c,j}/B}]\hat{\boldsymbol{p}}_{\boldsymbol{j}} \tag{35}$$

$$c_{\rho_j} = \frac{1}{m_j}(\hat{\boldsymbol{p}}_{\boldsymbol{j}}^T \boldsymbol{F}_G - k_j\rho_j - c_j\dot{\rho}_j - 2m_j\hat{\boldsymbol{p}}_{\boldsymbol{j}}^T[\tilde{\boldsymbol{\omega}}_{\mathcal{B}/N}]\boldsymbol{r}'_{P_{c,j}/B} - m_j\hat{\boldsymbol{p}}_{\boldsymbol{j}}^T[\tilde{\boldsymbol{\omega}}_{\mathcal{B}/N}][\tilde{\boldsymbol{\omega}}_{\mathcal{B}/N}]\boldsymbol{r}_{P_{c,j}/B}) \tag{36}$$

This same process is completed for the flexing equations. Equation (27) is manipulated to have $\ddot{\theta}_i$ isolated on the left-hand side of the equation:

$$\begin{aligned}\ddot{\theta}_i = {} & \frac{1}{(I_{s_{i,2}} + m_{\mathrm{sp}_i}d_i^2)}(-m_{\mathrm{sp}_i}d_i\hat{\boldsymbol{s}}_{i,3}^T\ddot{\boldsymbol{r}}_{B/N} - [(I_{s_{i,2}} + m_{\mathrm{sp}_i}d_i^2)\hat{\boldsymbol{s}}_{i,2}^T - m_{\mathrm{sp}_i}d_i\hat{\boldsymbol{s}}_{i,3}^T[\tilde{\boldsymbol{r}}_{H_i/B}]]\dot{\boldsymbol{\omega}}_{\mathcal{B}/N} \\ & -k_i\theta_i - c_i\dot{\theta}_i + \hat{\boldsymbol{s}}_{i,2}\cdot\boldsymbol{\tau}_{\mathrm{ext},H_i} + (I_{s_{i,3}} - I_{s_{i,1}} + m_{\mathrm{sp}_i}d_i^2)\omega_{s_{i,3}}\omega_{s_{i,1}} - m_{\mathrm{sp}_i}d_i\hat{\boldsymbol{s}}_{i,3}^T[\tilde{\boldsymbol{\omega}}_{\mathcal{B}/N}][\tilde{\boldsymbol{\omega}}_{\mathcal{B}/N}]\boldsymbol{r}_{H_i/B})\end{aligned} \tag{37}$$

Adhering to the general form introduced in Ref. [12], the equation is converted to

$$\ddot{\theta}_i = \boldsymbol{a}_{\theta_i}^T\ddot{\boldsymbol{r}}_{B/N} + \boldsymbol{b}_{\theta_i}^T\dot{\boldsymbol{\omega}}_{\mathcal{B}/N} + c_{\theta_i} \tag{38}$$

using the variables defined in Eqs. (39–41).

$$\boldsymbol{a}_{\theta_i} = -\frac{m_{\mathrm{sp}_i}d_i}{(I_{s_{i,2}} + m_{\mathrm{sp}_i}d_i^2)}\hat{\boldsymbol{s}}_{i,3} \tag{39}$$

$$\boldsymbol{b}_{\theta_i} = -\frac{1}{(I_{s_{i,2}} + m_{\mathrm{sp}_i}d_i^2)}[(I_{s_{i,2}} + m_{\mathrm{sp}_i}d_i^2)\hat{\boldsymbol{s}}_{i,2} + m_{\mathrm{sp}_i}d_i[\tilde{\boldsymbol{r}}_{H_i/B}]\hat{\boldsymbol{s}}_{i,3}] \tag{40}$$

$$c_{\theta_i} = \frac{1}{(I_{s_{i,2}} + m_{\mathrm{sp}_i}d_i^2)}(-k_i\theta_i - c_i\dot{\theta}_i + \hat{\boldsymbol{s}}_{i,2}\cdot\boldsymbol{\tau}_{\mathrm{ext},H_i} + (I_{s_{i,3}} - I_{s_{i,1}} + m_{\mathrm{sp}_i}d_i^2)\omega_{s_{i,3}}\omega_{s_{i,1}} \quad -m_{\mathrm{sp}_i}d_i\hat{\boldsymbol{s}}_{i,3}^T[\tilde{\boldsymbol{\omega}}_{\mathcal{B}/N}][\tilde{\boldsymbol{\omega}}_{\mathcal{B}/N}]\boldsymbol{r}_{H_i/B}) \tag{41}$$

The next step in the back-substitution method derivation [12] is to replace the second-order state variables for flexing and fuel slosh in the translational EOM, Eq. (16), with the definitions seen in Eqs. (33) and (38). Performing this step and combining like terms yields the decoupled translational EOM

$$\begin{aligned}&\left(m_{\mathrm{sc}}[I_{3\times3}] + \sum_{i=1}^{N_S} m_{\mathrm{sp}_i}d_i\hat{\boldsymbol{s}}_{i,3}\boldsymbol{a}_{\theta_i}^T + \sum_{j=1}^{N_P} m_j\hat{\boldsymbol{p}}_j\boldsymbol{a}_{\rho_j}^T\right)\ddot{\boldsymbol{r}}_{B/N} + \left(-m_{\mathrm{sc}}[\tilde{\boldsymbol{c}}] + \sum_{i=1}^{N_S} m_{\mathrm{sp}_i}d_i\hat{\boldsymbol{s}}_{i,3}\boldsymbol{b}_{\theta_i}^T + \sum_{j=1}^{N_P} m_j\hat{\boldsymbol{p}}_j\boldsymbol{b}_{\rho_j}^T\right)\dot{\boldsymbol{\omega}}_{\mathcal{B}/N} \\ &= m_{\mathrm{sc}}\ddot{\boldsymbol{r}}_{C/N} - 2m_{\mathrm{sc}}[\tilde{\boldsymbol{\omega}}_{\mathcal{B}/N}]\boldsymbol{c}' - m_{\mathrm{sc}}[\tilde{\boldsymbol{\omega}}_{\mathcal{B}/N}][\tilde{\boldsymbol{\omega}}_{\mathcal{B}/N}]\boldsymbol{c} - \sum_{i=1}^{N_S}(m_{\mathrm{sp}_i}d_i\dot{\theta}_i^2\hat{\boldsymbol{s}}_{i,1} + m_{\mathrm{sp}_i}d_ic_{\theta_i}\hat{\boldsymbol{s}}_{i,3}) - \sum_{j=1}^{N_P} m_jc_{\rho_j}\hat{\boldsymbol{p}}_j\end{aligned} \tag{42}$$

Completing the same method for the rotational EOM, Eq. (22), the decoupled rotational EOM can be seen in Eq. (43).

$$\begin{aligned}&\left[m_{\mathrm{sc}}[\tilde{\boldsymbol{c}}] + \sum_{i=1}^{N_S}(I_{s_{i,2}}\hat{\boldsymbol{s}}_{i,2} + m_{\mathrm{sp}_i}d_i[\tilde{\boldsymbol{r}}_{S_{c,i}/B}]\hat{\boldsymbol{s}}_{i,3})\boldsymbol{a}_{\theta_i}^T + \sum_{j=1}^{N_P} m_j[\tilde{\boldsymbol{r}}_{P_{c,j}/B}]\hat{\boldsymbol{p}}_j\boldsymbol{a}_{\rho_j}^T\right]\ddot{\boldsymbol{r}}_{B/N} + \left[[I_{\mathrm{sc},B}] + \sum_{i=1}^{N_S}(I_{s_{i,2}}\hat{\boldsymbol{s}}_{i,2}\right. \\ &\left. + m_{\mathrm{sp}_i}d_i[\tilde{\boldsymbol{r}}_{S_{c,i}/B}]\hat{\boldsymbol{s}}_{i,3})\boldsymbol{b}_{\theta_i}^T + \sum_{j=1}^{N_P} m_j[\tilde{\boldsymbol{r}}_{P_{c,j}/B}]\hat{\boldsymbol{p}}_j\boldsymbol{b}_{\rho_j}^T\right]\dot{\boldsymbol{\omega}}_{\mathcal{B}/N} = -[\tilde{\boldsymbol{\omega}}_{\mathcal{B}/N}][I_{\mathrm{sc},B}]\boldsymbol{\omega}_{\mathcal{B}/N} - [I'_{\mathrm{sc},B}]\boldsymbol{\omega}_{\mathcal{B}/N} \\ &-\sum_{i=1}^{N_S}\{(\dot{\theta}_i[\tilde{\boldsymbol{\omega}}_{\mathcal{B}/N}] + c_{\theta_i}[I_{3\times3}])(I_{s_{i,2}}\hat{\boldsymbol{s}}_{i,2} + m_{\mathrm{sp}_i}d_i[\tilde{\boldsymbol{r}}_{S_{c,i}/B}]\hat{\boldsymbol{s}}_{i,3}) + m_{\mathrm{sp}_i}d_i\dot{\theta}_i^2[\tilde{\boldsymbol{r}}_{S_{c,i}/B}]\hat{\boldsymbol{s}}_{i,1}\} - \sum_{j=1}^{N_P}(m_j[\tilde{\boldsymbol{\omega}}_{\mathcal{B}/N}][\tilde{\boldsymbol{r}}_{P_{c,j}/B}]\boldsymbol{r}'_{P_{c,j}/B} + m_jc_{\rho_j}[\tilde{\boldsymbol{r}}_{P_{c,j}/B}]\hat{\boldsymbol{p}}_j) + \boldsymbol{L}_B\end{aligned} \tag{43}$$

At this step, Eqs. (42) and (43) are only in terms of $\ddot{\boldsymbol{r}}_{B/N}$ and $\dot{\boldsymbol{\omega}}_{\mathcal{B}/N}$. Therefore, the translation and rotation EOMs can be written in the compact form seen in Eq. (44).

$$\begin{bmatrix}[A] & [B] \\ [C] & [D]\end{bmatrix}\begin{bmatrix}\ddot{\boldsymbol{r}}_{B/N} \\ \dot{\boldsymbol{\omega}}_{\mathcal{B}/N}\end{bmatrix} = \begin{bmatrix}\boldsymbol{v}_{\mathrm{trans}} \\ \boldsymbol{v}_{\mathrm{rot}}\end{bmatrix} \tag{44}$$

using the definitions in Eqs. (45–50).

$$[A] = m_{\text{sc}}[I_{3\times3}] + \sum_{i=1}^{N_S} m_{\text{sp}_i} d_i \hat{\boldsymbol{s}}_{i,3} \boldsymbol{a}_{\theta_i}^T + \sum_{j=1}^{N_P} m_j \hat{\boldsymbol{p}}_j \boldsymbol{a}_{\rho_j}^T \tag{45}$$

$$[B] = -m_{\text{sc}}[\tilde{\boldsymbol{c}}] + \sum_{i=1}^{N_S} m_{\text{sp}_i} d_i \hat{\boldsymbol{s}}_{i,3} \boldsymbol{b}_{\theta_i}^T + \sum_{j=1}^{N_P} m_j \hat{\boldsymbol{p}}_j \boldsymbol{b}_{\rho_j}^T \tag{46}$$

$$[C] = m_{\text{sc}}[\tilde{\boldsymbol{c}}] + \sum_{i=1}^{N_S} (I_{s_{i,2}} \hat{\boldsymbol{s}}_{i,2} + m_{\text{sp}_i} d_i [\tilde{\boldsymbol{r}}_{S_{c,i}/B}] \hat{\boldsymbol{s}}_{i,3}) \boldsymbol{a}_{\theta_i}^T + \sum_{j=1}^{N_P} m_j [\tilde{\boldsymbol{r}}_{P_{c,j}/B}] \hat{\boldsymbol{p}}_j \boldsymbol{a}_{\rho_j}^T \tag{47}$$

$$[D] = [I_{\text{sc},B}] + \sum_{i=1}^{N_S} (I_{s_{i,2}} \hat{\boldsymbol{s}}_{i,2} + m_{\text{sp}_i} d_i [\tilde{\boldsymbol{r}}_{S_{c,i}/B}] \hat{\boldsymbol{s}}_{i,3}) \boldsymbol{b}_{\theta_i}^T + \sum_{j=1}^{N_P} m_j [\tilde{\boldsymbol{r}}_{P_{c,j}/B}] \hat{\boldsymbol{p}}_j \boldsymbol{b}_{\rho_j}^T \tag{48}$$

$$\boldsymbol{v}_{\text{trans}} = m_{\text{sc}} \ddot{\boldsymbol{r}}_{C/N} - 2m_{\text{sc}}[\tilde{\boldsymbol{\omega}}_{\mathcal{B}/N}] \boldsymbol{c}' - m_{\text{sc}}[\tilde{\boldsymbol{\omega}}_{\mathcal{B}/N}][\tilde{\boldsymbol{\omega}}_{\mathcal{B}/N}] \boldsymbol{c} \quad - \sum_{i=1}^{N_S} (m_{\text{sp}_i} d_i \dot{\theta}_i^2 \hat{\boldsymbol{s}}_{i,1} + m_{\text{sp}_i} d_i c_{\theta_i} \hat{\boldsymbol{s}}_{i,3}) - \sum_{j=1}^{N_P} m_j c_{\rho_j} \hat{\boldsymbol{p}}_j \tag{49}$$

$$\begin{aligned} \boldsymbol{v}_{\text{rot}} = &-[\tilde{\boldsymbol{\omega}}_{\mathcal{B}/N}][I_{\text{sc},B}] \boldsymbol{\omega}_{\mathcal{B}/N} - [I'_{\text{sc},B}] \boldsymbol{\omega}_{\mathcal{B}/N} - \sum_{i=1}^{N_S} \{(\dot{\theta}_i [\tilde{\boldsymbol{\omega}}_{\mathcal{B}/N}] + c_{\theta_i} [I_{3\times3}])(I_{s_{i,2}} \hat{\boldsymbol{s}}_{i,2} + m_{\text{sp}_i} d_i [\tilde{\boldsymbol{r}}_{S_{c,i}/B}] \hat{\boldsymbol{s}}_{i,3}) \\ &+ m_{\text{sp}_i} d_i \dot{\theta}_i^2 [\tilde{\boldsymbol{r}}_{S_{c,i}/B}] \hat{\boldsymbol{s}}_{i,1}\} - \sum_{j=1}^{N_P} (m_j [\tilde{\boldsymbol{\omega}}_{\mathcal{B}/N}][\tilde{\boldsymbol{r}}_{P_{c,j}/B}] \boldsymbol{r}'_{P_{c,j}/B} + m_j c_{\rho_j} [\tilde{\boldsymbol{r}}_{P_{c,j}/B}] \hat{\boldsymbol{p}}_j) + \boldsymbol{L}_B \end{aligned} \tag{50}$$

The system of equations in Eq. (44) can be solved using the Schur matrix formulation [21] seen in Eqs. (51) and (52).

$$\dot{\boldsymbol{\omega}}_{\mathcal{B}/N} = ([D] - [C][A]^{-1}[B])^{-1} (\boldsymbol{v}_{\text{rot}} - [C][A]^{-1} \boldsymbol{v}_{\text{trans}}) \tag{51}$$

$$\ddot{\boldsymbol{r}}_{B/N} = [A]^{-1} (\boldsymbol{v}_{\text{trans}} - [B] \dot{\boldsymbol{\omega}}_{\mathcal{B}/N}) \tag{52}$$

The remaining step to solve the system of EOMs is to back-substitute the values for $\dot{\boldsymbol{\omega}}_{\mathcal{B}/N}$ and $\ddot{\boldsymbol{r}}_{B/N}$ into Eqs. (33) and (38) and solve for all of the second-order derivatives of the flexing and fuel slosh states. This back-substitution method for solving the system of EOMs is shown to be beneficial from a software architecture perspective [12], but the computational performance of this method needs to be evaluated. Note that this analytical back-substitution is quite complex in its algebra, and thus the speed improvements over doing a full system mass matrix inversion are of interest. The more complex effectors such as the hinged panels require more algebra than the simpler fuel slosh particles.

IV. Back-Substitution Method Computational Performance

The resulting formulation for the back-substitution method removes the necessity of inverting the system mass matrix and only requires two 3×3 matrix inversions using the Schur matrix formulation seen in Eqs. (51) and (52). This form of the solution is the same regardless of the system being considered as long as it adheres to the form seen in Ref. [12]. This results in a fixed-size matrix implementation in software. In contrast, in solutions having to populate a full system mass matrix, the mass matrix can change in size, which results in dynamically sized matrices that can impact computational performance. The size of this matrix inversion is $N_S + N_P + 6$, where N_S is the number of flexing bodies and N_P are the number of sloshing particles.

To analyze these effects with respect to computational performance, a simulation is created to attach a varying number of fuel slosh particles and flexing appended bodies to see how the performance scales with respect to the number of degrees of freedom. The software implementation of this simulation was verified using energy and momentum conservation techniques, and the results can be seen in Fig. 3. Both the back-substitution method introduced in this paper for this system and the full system matrix solution are considered in this analysis. The specific spacecraft parameters for the hub, fuel slosh, and flexing appended bodies are not included here because the computational performance is independent of these parameters. The associated mathematical operations are the critical component, not the numerical values being computed.

A computationally efficient C++ library named *Eigen* [22] is used for all of the matrix algebra. Eigen includes different methods to solve a system of equations. One of them, widely known as QR decomposition, does not require the solution of the system mass matrix inverse, but rather solves directly for the solution to the system [22]. The QR decomposition method is chosen for this comparison. The QR decomposition method requires $(4/3)N^3$ operations, where N is the size of the matrix [23]. Other methods, such as LU decomposition that scales with $(2/3)N^3$ operations, could also have been used. However, the important discussion in this paper is how the back-substitution method computational efficiency scales with the number of degrees of freedom of the system. The QR decomposition method is chosen purely as a benchmark.

The computational performance results are illustrated in Fig. 4. The quantity used to define the performance is the times longer for the system mass matrix solution. Therefore, the higher the number, the more efficient the back-substitution method is. Also, it should be noted that the figure uses an interpolation function to try and smooth the curves between the different data points. The data points are discrete integer values representing the number of fuel slosh particles and solar panels, and so the discontinuities are expected. The results show that at a minimum the back-substitution method is three times as fast and the speed improvements positively scale with the number of attached fuel slosh particles and flexing appended bodies. When there are 10 fuel slosh particles and 10 appended flexing bodies, the system mass matrix solution takes 8 times

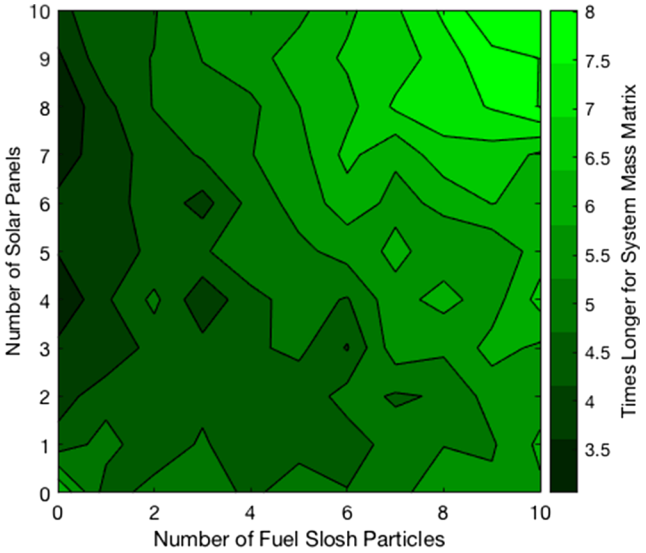

Fig. 4 Computational efficiency of back-substitution method.

longer to compute the solution. The back-substitution method is always more efficient because a dynamically allocated size matrix is not required for this solution. The reason that the number of solar panels does not scale as quickly as fuel slosh particles is because of the complexity of the EOMs. There are more calculations required when implementing the flexing equations than the fuel slosh equations; therefore, the speed up does not scale as quickly as the fuel slosh. These results quantify the expected computational performance of the back-substitution method and furthers the applicability of the back-substitution method for complex spacecraft simulations.

It should be noted that there are techniques available to increase the computational efficiency of solutions of systems of equations depending on the form of the system mass matrix. For example, one method is to ignore small-order effects from certain degrees of freedom in your system [23]. This approximation reduces the size of your system mass matrix, thus making the solution more computationally efficient. The back-substitution method also allows for this type of approximation. A powerful aspect of the back-substitution method is that the analytical expressions of the EOMs are available, and therefore there is precise tuning available depending on the application. The key takeaway from this paper is showing that the back-substitution method is computationally more efficient than the QR decomposition method, which serves as a benchmark comparison. The increased computational performance is an additional attribute to the modularity of the back-substitution method discussed in Ref. [12].

V. Conclusions

The back-substitution method introduced in Ref. [12] modularizes the equations of motion for multibody spacecraft dynamics problems, and a modular software architecture is presented using this method. It is shown to be beneficial from a software architecture perspective; however, the computational efficiency is needed to be quantified. This paper analyzes the computational performance of the back-substitution method for a spacecraft with a general number of fuel slosh particles and flexing solar arrays and confirms that the back-substitution method is more computationally efficient than solving the system of equations using a QR decomposition to solve the system of equations. For this system the back-substitution method is at least three times more efficient because the system does not require a dynamically allocated matrix, and the performance shows to positively scale with the number of fuel slosh particles and appended flexing bodies. With 10 appended bodies and 10 fuel slosh particles, the back-substitution method is 8 times more efficient. The computational performance gain shows to grow at a faster rate with the fuel slosh particles than the flexing appended bodies because the fuel slosh particles require less computation to be completed. These results demonstrate that the back-substitution method is not only more convenient and maintainable from a software architecture point of view [12], but also computationally efficient for simulating multibody spacecraft dynamics.

References

[1] Banerjee, A. K., "Contributions of Multibody Dynamics to Space Flight: A Brief Review," *Journal of Guidance, Control, and Dynamics*, Vol. 26, No. 3, 2003, pp. 385–394. doi:10.2514/2.5069

[2] Junkins, J., and Kim, Y., *Introduction to Dynamics and Control of Flexible Structures*, AIAA Education Series, AIAA, Washington, D.C., 1993, Chap. 4. doi:10.2514/4.862076

[3] Angeles, J., and Kecskeméthy, A., *Kinematics and Dynamics of Multi-Body Systems*, Vol. 360, CISM, Udine, 2014, Chap. 3. doi:10.1007/978-3-7091-4362-9

[4] Kane, T. R., and Levinson, D. A., "Formulation of Equations of Motion for Complex Spacecraft," *Journal of Guidance, Control, and Dynamics*, Vol. 3, No. 2, 1980, pp. 99–112. doi:10.2514/3.55956

[5] Likins, P. W., "Point-Connected Rigid Bodies in a Topological Tree," *Celestial Mechanics*, Vol. 11, No. 3, 1975, pp. 301–317. doi:10.1007/BF01228809

[6] Jerkovsky, W., "The Structure of Multibody Dynamics Equations," *Journal of Guidance, Control, and Dynamics*, Vol. 1, No. 3, 1978, pp. 173–182. doi:10.2514/3.55761

[7] Jeffreys, H., and Jeffreys, B., *Methods of Mathematical Physics*, Cambridge Mathematical Library, Cambridge Univ. Press, Cambridge, United Kingdom, 1999, Chap. 9. doi:10.1002/9783527617210

[8] Jain, A., and Rodriguez, G., "Diagonalized Lagrangian Robot Dynamics," *IEEE Transactions on Robotics and Automation*, Vol. 11, No. 4, 1995, pp. 571–584. doi:10.1109/70.406941

[9] Forbes, J. R., "Identities for Deriving Equations of Motion Using Constrained Attitude Parameterizations," *Journal of Guidance, Control, and Dynamics*, Vol. 37, No. 4, 2014, pp. 1283–1289.
doi:10.2514/1.G000221
[10] Rodriguez, G., and Jain, A., "Spatial Operator Algebra for Multibody System Dynamics," *Journal of the Astronautical Sciences*, Vol. 40, Jan.–March 1992, pp. 27–50.
doi:10.1177/027836499101000406
[11] Jain, A., and Rodriguez, G., "Recursive Flexible Multibody System Dynamics Using Spatial Operators," *Journal of Guidance, Control, and Dynamics*, Vol. 15, No. 6, 1992, pp. 1453–1466.
doi:10.2514/3.11409
[12] Allard, C., Ramos, M. D., Schaub, H., Kenneally, P., and Piggott, S., "Modular Software Architecture for Fully Coupled Spacecraft Simulations," *Journal of Aerospace Information Systems*, Vol. 15, No. 12, 2018, pp. 670–683.
doi:10.2514/1.I010653
[13] Kuang, J., Meehan, P. A., Leung, A., and Tan, S., "Nonlinear Dynamics of a Satellite with Deployable Solar Panel Arrays," *International Journal of Non-Linear Mechanics*, Vol. 39, No. 7, 2004, pp. 1161–1179.
doi:10.1016/j.ijnonlinmec.2003.07.001
[14] Wallrapp, O., and Wiedemann, S., "Simulation of Deployment of a Flexible Solar Array," *Multibody System Dynamics*, Vol. 7, No. 1, 2002, pp. 101–125.
doi:10.1023/A:1015295720991
[15] Wie, B., Furumoto, N., Banerjee, A., and Barba, P., "Modeling and Simulation of Spacecraft Solar Array Deployment," *Journal of Guidance, Control, and Dynamics*, Vol. 9, No. 5, 1986, pp. 593–598.
doi:10.2514/3.20151
[16] Abramson, H., "The Dynamic Behavior of Liquids in Moving Containers," NASA SP-106, 1966.
[17] Kana, D. D., "A Model for Nonlinear Rotary Slosh in Propellant Tanks," *Journal of Spacecraft and Rockets*, Vol. 24, No. 2, March 1987, pp. 169–177.
[18] Allard, C., Diaz-Ramos, M., and Schaub, H., "Spacecraft Dynamics Integrating Hinged Solar Panels and Lumped-Mass Fuel Slosh Model," *AIAA/AAS Astrodynamics Specialist Conference*, AIAA Paper 2016-5684, 2016.
doi:10.2514/6.2016-5684
[19] Kane, T. R., and Levinson, D. A., "Multibody Dynamics," *Journal of Applied Mechanics*, Vol. 50, No. 4b, 1983, pp. 1071–1078.
doi:10.1115/1.3167189
[20] Schaub, H., and Junkins, J. L., *Analytical Mechanics of Space Systems*, 3rd ed., AIAA Education Series, AIAA, Reston, VA, 2014.
doi:10.2514/4.102400
[21] Zhang, F., *The Schur Complement and Its Applications*, Springer, Boston, MA, 2005.
doi:10.1007/b105056
[22] "Eigen: A C++ Template Library for Linear Algebra: Matrices, Vectors, Numerical Solvers, and Related Algorithms," Aug. 2016, http://eigen.tuxfamily.org.
[23] Trefethen, L. N., and Bau, D., *Numerical Linear Algebra*, SIAM, Philadelphia, PA, 1997, Chap. 2.

J. P. How
Associate Editor